

THERMOLUMINESCENCE EXCITATION SPECTROSCOPY:
A TECHNIQUE TO STUDY ENERGY LEVELS OF IMPURITY IN SOLIDS

by

JIANWEI WANG

(Under the Direction of UWE HAPPEK)

ABSTRACT

This thesis presents a technique to locate the ground state of impurity ions relative to the host conduction band, using thermoluminescence. The technique makes use of the concept that thermoluminescence probes the occupation of electron traps, and the fact that these traps are filled via promotion of impurity electrons into the conduction band. Using tunable radiation we determine the threshold for trap filling, which is given by the ionization threshold of the impurity. This technique is a form of excitation spectroscopy, sensitive to electron (or hole) transport processes in solids. Advantages of thermoluminescence excitation spectroscopy over complementary techniques, such as photoconductivity, include impurity specific signals, applicability to both bulk and power samples, and high sensitivity.

INDEX WORDS: Thermoluminescence, Photoionization, Excitation spectroscopy

THERMOLUMINESCENCE EXCITATION SPECTROSCOPY:
A TECHNIQUE TO STUDY ENERGY LEVELS OF IMPURITY IN SOLIDS

by

JIANWEI WANG

B.Eng., Tianjin University, P. R. China 1992

A Thesis Submitted to the Graduate Faculty of The University of Georgia in Partial
Fulfillment of the Requirements for the Degree

MASTER OF SCIENCE

ATHENS, GEORGIA

2002

© 2002

Jianwei Wang

All Rights Reserved

THERMOLUMINESCENCE EXCITATION SPECTROSCOPY:
A TECHNIQUE TO STUDY ENERGY LEVELS OF IMPURITY IN SOLIDS

by

JIANWEI WANG

Approved:

Major Professor: Uwe Happek

Committee: William M. Dennis
W. Gary Love

Electronic Version Approved:

Gordhan L. Patel
Dean of the Graduate School
The University of Georgia
May 2002

ACKNOWLEDGMENTS

I am very glad to have this page for my appreciations to many people who contributed to making this thesis possible.

First, I would like to thank my advisor Dr. Uwe Happek for giving me this great opportunity to learn Physics and make the learning into the actual research experiments.

Second, I wish to thank my fellow student Jay Fleniken. We work together. He gives me a lot helps in my experiment, from initial introduction, experimental setup and procedure, to theory discussion and final thesis. His suggestion is pretty valuable.

Third, I would like to thank all my fellow students in the Physics Department and all my friends in the University of Georgia. They make my life in Athens more enjoyable.

I have to mention that Professor William Yen is my original advisor. I am sorry that I could not continue to study under his guidance because of his sick. Thanks for his initial support and help.

Finally, I wish to thank my beloved wife Wang Xin. Her supports let me truly understand the meaning of family. My love for her is boundless.

TABLE OF CONTENTS

	Page
ACKNOWLEDGMENTS.....	iv
CHAPTER	
1 INTRODUCTION.....	1
2 BACKGROUND REVIEW	3
2.1 Impurity Energy Levels.....	3
2.2 Calculations of Photoionization Threshold.....	4
2.3 Electron Transfer Processes and Born-Harber Cycle.....	4
2.4 Photoelectron Spectroscopy	9
2.5 Photoconductivity.....	12
3 INTRODUCTION OF THERMOLUMINESCENCE.....	16
3.1 What is the Thermoluminescence?	16
3.2 Basic Backgrounds of Luminescence	17
3.3 Simple Model for Thermoluminescence	20
3.4 Analysis of Simple Model.....	22
4 THERMOLUMINESCENCE EXPERIMENT.....	26
4.1 Basic Idea	26
4.2 Experimental Setup and Procedure	30
4.3 Experimental Results	32
5 CONCLUSIONS.....	43
REFERENCES.....	45

CHAPTER 1

INTRODUCTION

The impurities in solids give rise to the generation of new optical absorption bands, generally introduce some energy levels in the forbidden gap between the extended electronic states of the host lattice, i.e. the valence and the conduction bands. The optical properties of solids are determined by these levels of the impurities.

The rare earth ions are characterized by an incompletely filled 4f shell. The 4f orbital lies inside the ion and is shielded from the surroundings by the filled $5s^2$ and $5p^6$ orbitals. Therefore the influence of the host on the optical transitions within the $4f^n$ configuration is small [1]. It has been customary to consider the impurity electrons independently from the environment with the exception of the coupling to the lattice vibration. The influence on impurity electrons by host environment comes from the crystal field of certain symmetry and strength, which gives rise to the energy splitting and shifting of the free ion orbitals [2]. Therefore the major optical properties of rare earth activated solids are determined by the intra-ion f-f and f-d transitions that are weakly perturbed by the surrounding of the host system. Observing the transitions among the crystal field split levels has been the main subject of the impurity spectroscopy of the solids. However, for a global understanding of the optical properties of a doped solid, we have to include the excitation processes that involve both the impurity electrons states and the extended electronic states of the host lattice. The importance of this for describing the luminescence properties of doped solids has become increasingly evident. It is partly related to the rising activity in scintillator and phosphor research where the applications of such impurity-activated systems require excitation energies larger than the

bandgap of a material [1]. The excitation of an impurity ion often involves the actual movement of a charge over an inter-ionic distance and the corresponding processes are called electron transfer processes. To describe the impurity-host system and electron transfer processes, a donor-acceptor model is used, which is used extensively for doped semiconductors [3, 4].

Electron transfer processes play an important role in phosphors and scintillators, photovoltaic and photorefractive materials, spectral (chemical) holeburning, and can influence the efficiency of solid lasers via excited state absorption. In these and other examples the location of the impurity ground state relative to the host valence and conduction band is an important factor. Photoelectron spectroscopy measures directly the electron density as a function of binding energy, providing, in principle, the energy levels of both host and impurity ions [5]. Photoconductivity is another technique that allows one to determine the position of impurity energy levels with respect to the host bands. Our group has applied this method to study a number of systems [6, 7, 8, 22].

In the present thesis we attempt to present a complementary technique that uses thermoluminescence to locate the impurity energy levels relative to the host bands. Thermoluminescence is the thermally stimulated emission of light following an earlier absorption of energy from radiation. A typical application of thermoluminescence is the study of trap depth [9]. In our application, we are not interested in the location of the traps, but simply use traps as an indicator for impurity electrons promotion into the conduction band.

CHAPTER 2

BACKGROUND REVIEW

2.1 Impurity Energy Levels

From the energy band theory of solids [10], the allowed energies for the electrons lie only in “allowed zones” (called energy band). Between energy bands are “forbidden zones”(called energy gap). There is no energy level in energy gap. The electrons can only stay in those allowed energy bands. However, if there are impurities in the solid, some discrete energy levels may be formed within the forbidden energy gap. These energy levels are called localized energy levels.

The appearance of foreign impurities in a solid leads to local disturbances in the periodicity of the potential field. If one denotes the potential function of a perfect lattice by $V(r)$, then, in the presence of impurities, the potential will be $V(r) = V_0(r) + V'(r)$. The second term differs from zero in a particular volume in the vicinity of the impurity.

If we assume that $V'(r)$ is determined by the Coulomb interaction of the electron with the point charge of the impurity, i.e., $V'(r) = -e^2 / \epsilon r$ where ϵ is the dielectric constant of matter, the Schrodinger equation for such a model is reduced to the equation for the hydrogen atom. The energy of bound states will be given by

$$E_n = -\frac{m_e (e_e^*)^4}{2\hbar^2 n^2} = -\frac{m_e^4}{2\hbar^2 n^2 \epsilon^2} \left(\frac{m_e}{m} \right) = -\frac{13.6}{n^2 \epsilon^2} \left(\frac{m_e}{m} \right) eV \quad (2.1)$$

Where e^* is the effective charge of the electron, m is the electron mass in vacuum, and n is the principal quantum number. Since in deriving this relation it was assumed that the energy of the conduction band bottom was equal to zero, it follows from equation (2.1) that the electron near impurity has levels lying in the forbidden band. Equation (2.1) is

also valid for the energy of holes near the impurity if one replaces m_e by the effective mass m_h of the hole, sets the energy of the valence band top equal to zero, and assumes that the energy increases with increasing depth of the valence band [38].

2.2 Calculations of Photoionization Threshold

Christian [39] gave a simple way to calculate the photoionization threshold, i.e., the minimum energy difference between the ground state of impurity ion and the bottom of the conduction band; also compared the values calculated with the data experimentally measured and had a good fit.

The photoionization energy of the impurity ion E_{PI} can be expressed as follow:

$$E_{PI} = I - C \quad (2.2)$$

Where I represents the ionization potential of the free impurity ion, C is the correction of I due to the effect of the crystal surroundings.

The simplest theory of C is that it equals the electrostatic energy E_M (called the Madelung energy) at a metal site in the crystal. However, the actual nearest neighbor ion positions around an impurity ion have a shift from the theoretical positions. This shift has an appreciable effect on the Madelung energy at the metal site. Therefore, the corrections ΔE_M of the Madelung energy are necessary and can be calculated simply for the change in the near neighbor distance. Furthermore, the actual calculation should take account of the electronic polarization of the lattice during the ionization process.

At last, the equation (2.2) for the photoionization energy of impurity ion becomes:

$$E_{PI} = I + E_M + \Delta E_M - E_{PM} \quad (eV) \quad (2.3)$$

Where E_{PM} is the polarization energy.

2.3 Electron Transfer Processes and Born-Haber Cycle

From above, we reach the situation where there are localized impurity energy levels present in the energy gap in addition to the delocalized states belonging to the

valence and conduction bands of the host. For a stable impurity ion (M^{n+}) with a ground state located within the host band gap, in the presence of the incident radiation of energy, the following simplified electron transfer processes may take place (as shown schematically in figure 2.1).

a) Absorbing the incident energy at $h\nu_a \geq E_g$ promotes an electron across the energy gap E_g from valence band to the conduction band, creating both a free hole and a free electron (transition 1).

b) Absorbing the incident energy at $h\nu_b$ leads to a transition between two localized energy levels: the ground state and excited state (M^{n+})* of an impurity. The excitation is followed by radiative or nonradiative relaxation to the ground state at the same or at some neighboring impurity site (transition 2 and 3).

c) Absorbing the incident energy at $h\nu_c = h\nu_{CT}$ gives rise to the transfer of a valence band electron to an empty impurity ion level (transition 4). This process leaves a hole in the host valence band. Since in this process the impurity ion accepts an electron ($M^{n+} \rightarrow M^{(n-1)+}$) it is called an acceptor-like charge transfer process (CT).

d) Absorbing the incident energy at $h\nu_d$ leads to the transfer of an electron from a filled impurity state to the conduction band (transition 5). This process ionizes the impurity ion ($M^{n+} \rightarrow M^{(n+1)+}$) and since the electron is donated to the host conduction band it is called a donor-like charge transfer or photoionization (PI).

What we are interested in is the processes c) and d). The difference between them is often (but not only) made by means of an electrical measurement that detects freely moving charge carriers in the lattice. Apart from the different conductivity mechanism, the sign of the charge carriers can be determined using the Hall effect [11]. The processes b) and c) can be analyzed by the Born-Haber cycle, which is named after the German physicist Max Born and chemist Fritz Haber [12,13]. Originally, it described a method of

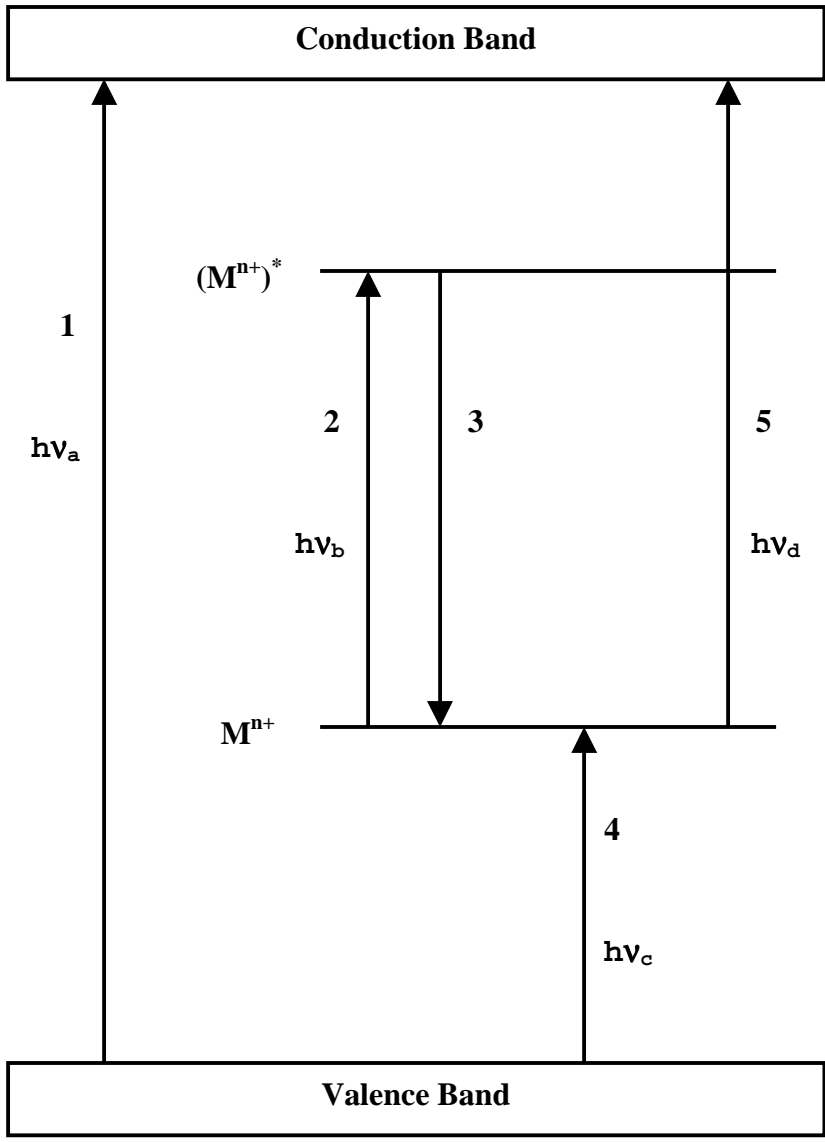


Figure 2.1. Electron transfer processes

estimation the cohesive energy of ionic lattices. The approach is based on thermodynamic principles only, with no specific impurity or host features involved, which makes it very general and applicable to any impurity in any host. The Born-Haber cycle was further developed by McClure and co-workers to find the relationship between photoionization and charge transfer processes of impurity ions [14].

Applying the donor-acceptor model to a trivalent rare earth impurity RE^{3+} , figure 2.2 shows the location of the highest occupied 4f ground state level within the energy band of the host. The host valence band and conduction band are separated by E_G . The photon energy for a donor process ($RE^{3+} \rightarrow RE^{4+} + e^-$), i.e. promoting the electron from the highest occupied ground state level to the conduction band is given by $h\nu_d > E_{CB}$, where E_{CB} is the energy difference between the bottom of the conduction band and the rare earth ground state. This process leaves the rare earth ion in the tetravalent state. The RE^{4+} ion can be converted back to a RE^{3+} ion in an acceptor-like process ($RE^{4+} \rightarrow RE^{3+} + e^+$) by transferring an electron from the valence band to the 4f shell of the RE^{4+} ion, thus converting RE^{4+} to RE^{3+} . As a result, this electron will occupy the highest filled f-level of the RE^{3+} ground state configuration, leaving a hole (e^+) in the valence band. Thus the photon energy for an acceptor process is given by $h\nu_c > E_{VB}$, where E_{VB} is the energy difference between the highest occupied 4f ground state level of the RE^{3+} ion and the top of the valence band. It becomes evident from figure 2.2 that E_{CB} , E_{VB} and E_G are related through

$$E_G = E_{CB} + E_{VB} \quad (2.4)$$

Which states that the energies for the donor and acceptor like electron transfer processes add up to the value of the energy gap the host material. It is to be emphasized that this relation is valid for the relaxed thermodynamic states at $T = 0$ K, corresponding to zero

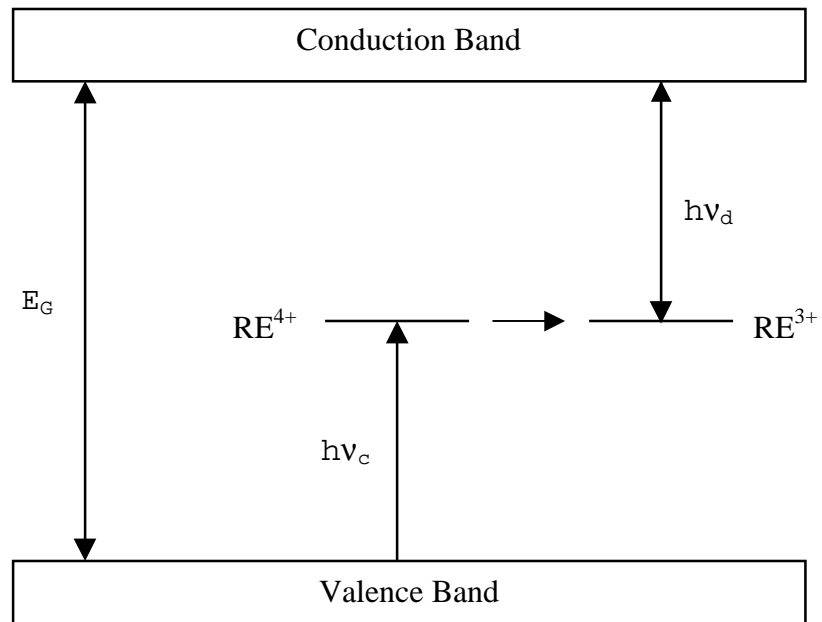


Figure 2.2. Donor and acceptor like electron transfer processes for a trivalent rare earth impurity RE^{3+} .

phonon transition. Thus, direct comparison with experimental data is not always straightforward. Special corrections must be made.

As a conclusion, if we know two of the three energy values (E_{CB} , E_{VB} and E_G) from the experimental results, the third one can be estimated with corrections. Therefore, the situation of impurity energy levels can be obtained.

We investigate a method that uses thermoluminescence to give the ionization threshold of impurity ion in solid (E_{VB}). The details are described in the later sections.

2.4 Photoelectron Spectroscopy

Photoelectron spectroscopy is an old experimental technique that is still in extensive use [15]. It utilizes a monochromatic source of photons to eject photoelectrons, thereby learning about electronic structure of a sample through data on binding energies. This method is based upon the photoelectronic effect, which was detected by Hertz in 1887 [16]. Einstein in 1905 was able to explain this phenomenon by involving the quantum nature of light [17].

The basic photoelectron spectroscopic technique involves photo-ionization of the sample atom or molecule A by a beam of monoenergetic photons, in which process the sample loses an electron:



$h\nu$ is the energy of a photon given by the Einstein relation. A^+ is the resulting ion formed in the state with internal energy $E(A^+)$, and e^- is the product photoelectron. Conservation of energy then requires that:

$$E(A) + h\nu = E(A^+) + E(e^-) \quad (2.6)$$

Since the electron's energy is present solely as kinetic energy (KE), equation (2.4) can be rearranged to give the following expression for the KE of the photoelectron:

$$KE = h\nu - (E(A^+) - E(A)) \quad (2.7)$$

The final term in brackets, representing the difference in energy between the ionized and neutral atom, is generally called the binding energy (BE) of the electron- this then leads to the following commonly quoted equation:

$$KE = h\nu - BE \quad (2.8)$$

Conventionally the binding energies (BE) of energy levels in solids are measured with respect to the Fermi-level of solid, rather than the vacuum level. The equation (2.6) must have a small correction:

$$KE = h\nu - BE - \Phi \quad (2.9)$$

Where Φ is the work function that is the energy difference between the Fermi-level and vacuum level.

However, the incident ionization photons can do more than remove the most loosely bound electron. If the photon energy is sufficiently high, it can also remove the tightly bound electrons. As a result, the ejected electrons have different kinetic energies; therefore have different binding energy according to the equation (2.7). When the ejected electrons are detected in an energy analyzer, the expected electron kinetic energy spectrum is an energy distribution curve (EDC). From EDC we can figure out the electric structure of the sample.

The schematic setup for modern photoelectron spectroscopy experiment is shown in figure 2.3. The light impinges on the sample. The photoelectrons excited are analyzed with respect to their kinetic energies in an electrostatic analyzer. Knowing the energy of the light and the work function, one can determine the binding energy of the electrons in the sample by the equation (2.7).

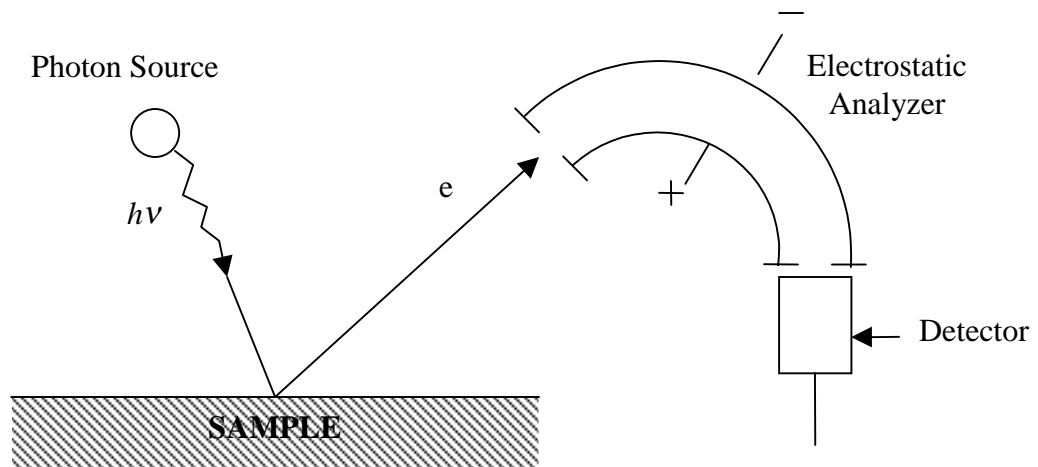


Figure 2.3. Schematic setup for a photoelectron spectroscopy experiment.

2.5 Photoconductivity

Photoconductivity is defined as the transient change of the electrical conductivity associated with the absorption of light by a solid. The first observation of this effect was reported in 1873 by W. Smith in Nature [18].

Photoconductivity is a powerful tool to study the delocalized transitions in doped solids [11,19]. This experimental technique allows the determination of the position of impurity energy levels with respect to the conduction and valence bands. Traditionally, this method has been used in semiconductor physics, but a similar, although refined approach, can be applied to insulators as well. In practice, for the proper interpretation of photoconductivity data it is almost always necessary to complement photoconductivity spectra by standard absorption and photoexcitation techniques. Photoconductivity is a powerful method that provides extremely useful information especially for non-luminescence systems where emission based information about the system cannot be obtained. McClure and coworkers have used this technique to determine the positions of impurity energy levels in the host lattice energy band in a variety of systems [14, 20, 21].

The schematic setup for a photoconductivity experiment is shown in figure 2.4. Scanning the energy of light incident on a sample will change the nature of induced electron transfer processes like mentioned before (section 2.2). Above a practical value of photon energy, the resulting electronic transition does not occur just on the impurity ion but involves one or both of the host bands. Free electrons created in the conduction band or holes created in the valence band can give rise to a current when an applied external electric field is introduced into the random thermal motion of charge carriers. An example of a photoconductivity spectrum is shown in figure 2.5. It is the photoconductivity spectra for CaS: 0.7% Eu powder. From the figure, we find there are two thresholds at low temperature ($T = 80\text{K}$): one about 650nm and the second around 510nm. We have

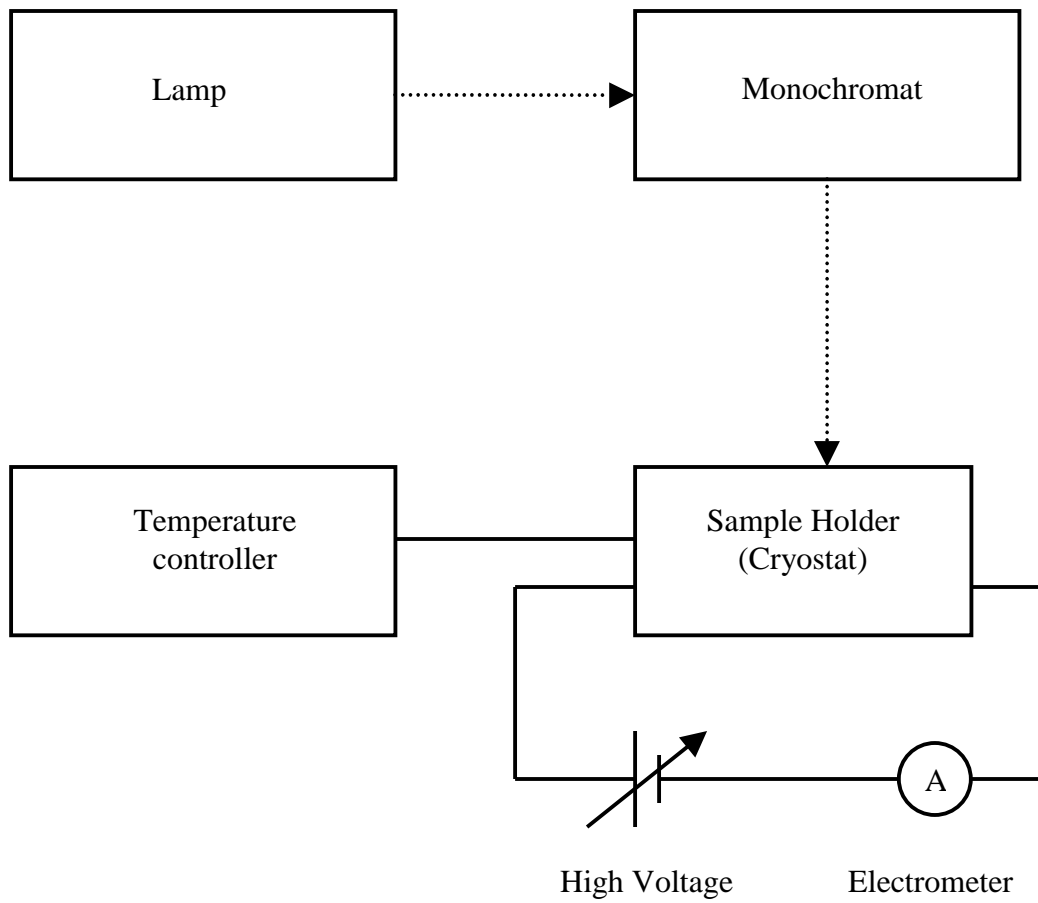


Figure 2.4. Schematic setup for photoconductivity measurements

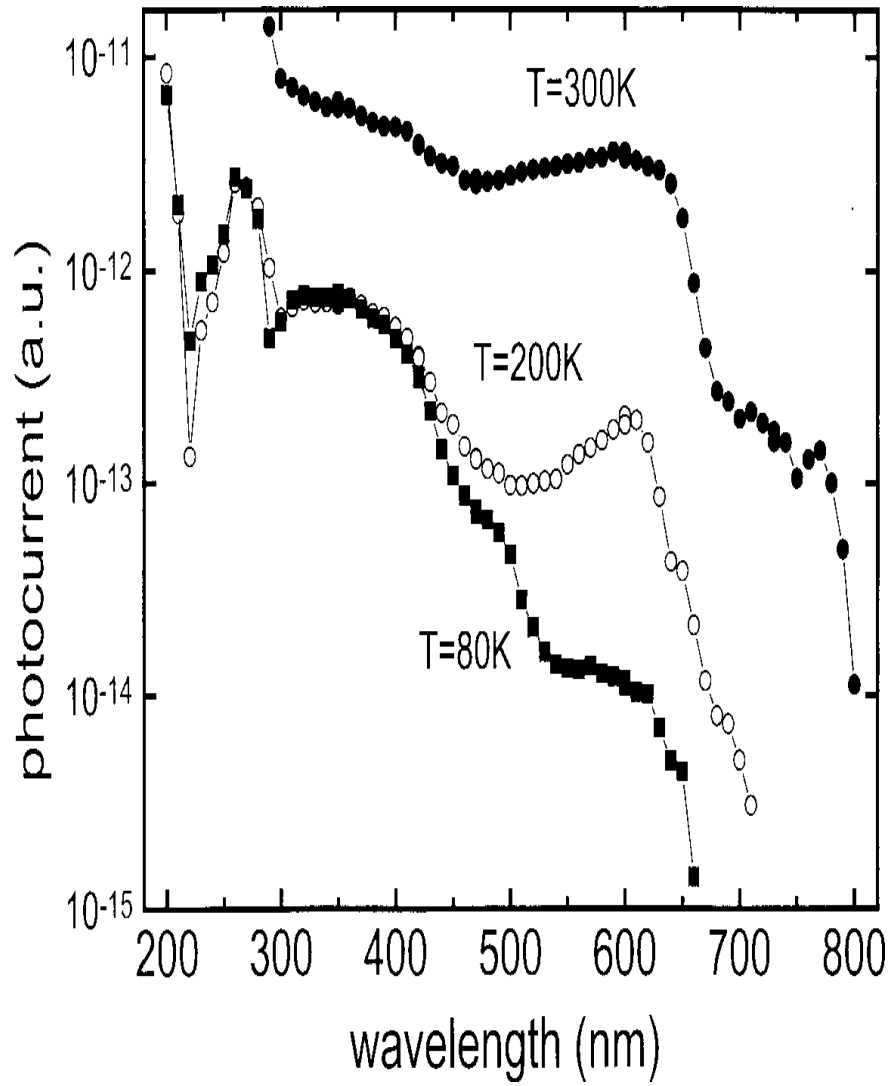


Figure 2.5. Photoconductivity spectra for CaS: 0.7% Eu powder at different temperatures.

interpreted the rise at 510nm as a direct excitation of a Eu^{2+} ion to the conduction band [22]. Therefore, we can know the situation of the energy levels of impurity ion Eu^{2+} in CaS. The details of interpretation will be given in the chapter four.

CHAPTER 3

INTRODUCTION OF THERMOLUMINESCENCE

3.1 What is the Thermoluminescence?

It is difficult to point exactly when the word “thermoluminescence” was first used in the published literature, but it is certainly used in 1895 by Wiedemann & Schmidt [23].

Thermoluminescence is defined as the emission of light during heating of a solid following the previous absorption of energy during irradiation. From the term, thermoluminescence, one may consider that heating is the main energy source of the luminescence. But in fact, it is not the case and quite different from the radiation spontaneously emitted from a substance when it is heated to incandescence. The essential condition for thermoluminescence to occur in a solid is that the material must have been previously exposed to radiation. This radiation is the source of energy; whereas the heating is just a trigger to help release the absorbed energy. So, the term “Thermally Stimulated Luminescence” is more accurate; however, “thermoluminescence” has become the common term.

Here, a particular feature of thermoluminescence has to be mentioned. That is, once thermoluminescence emission is observed, the material cannot be made to emit it again by simply cooling the specimen and reheating. The material has to be re-exposed to radiation; raising the temperature will then result in thermoluminescence emission again.

Thermoluminescence is just one type of luminescence phenomena. The fundamental principles of thermoluminescence are essentially the same as those that govern all luminescence processes.

3.2 Basic Backgrounds of Luminescence

Luminescence is the light emission from a material following the initial absorption of external energy. Depending on the characteristic lifetime τ between absorption of the excitation energy and emission of the luminescence, one can distinguish two classes of luminescence—fluorescence and phosphorescence. The line of mark is about 10^{-8} s [24, 25]. This very short time means that the fluorescence emission is essentially a spontaneous process. It takes place simultaneously with the absorption of radiation and stops immediately when the radiation ceases, as shown in figure 3.1. On the other hand, the phosphorescence emission is characterized by a delay between the radiation absorption and the time t_{\max} to reach full intensity. Also, in figure 3.1 the phosphorescence is seen to continue for some time after the excitation has been removed. Phosphorescence and thermoluminescence are the same process; the only difference is the fixed and the rising temperature, respectively, of the emitting material during the emission.

According to the Jablonski model [26], consider a ground state energy level g and an excited state level e , illustrated in figure 3.2(a). Energy from radiation is transferred to the electrons of the solid, thus exciting the electrons from g to e (transition 1). Fluorescence takes place when an electron returns to level g (transition 2). The delay between excitation and emission is less than 10^{-8} s. However, if the excited electron makes a transition from the excited state to a metastable level m (transition 3 in figure 3.2(b)), where it will remain until it receives enough energy to return to the excited state e (transition 4) with the subsequent emission of light. The return to the ground state is delayed much longer and in this case the process is known as phosphorescence.

Like mentioned above, the electron in the metastable energy level needs to absorb enough energy to go back to the ground state e . If we give the energy by heating the

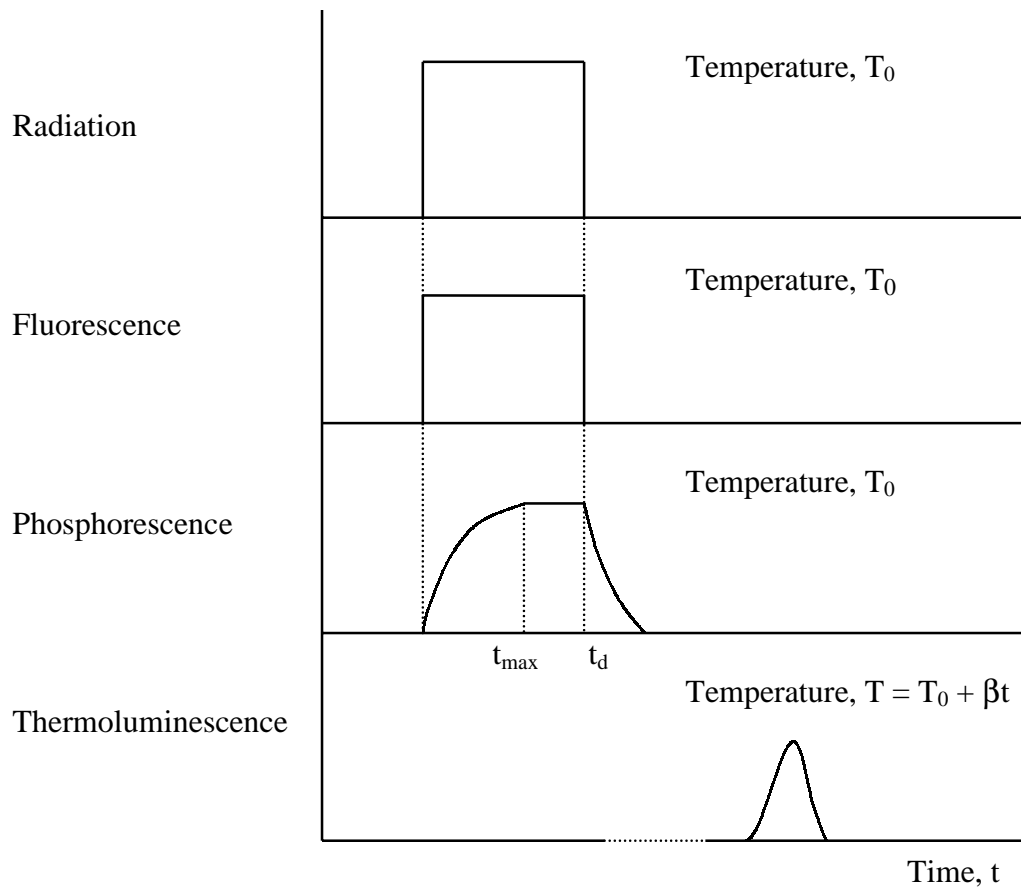


Figure 3.1. Relationships between radiation and the emission of fluorescence, phosphorescence and thermoluminescence. T_0 is the temperature at which radiation takes place; β is the heating rate; t_d is the time at which the radiation ends and the decay of phosphorescence begins.

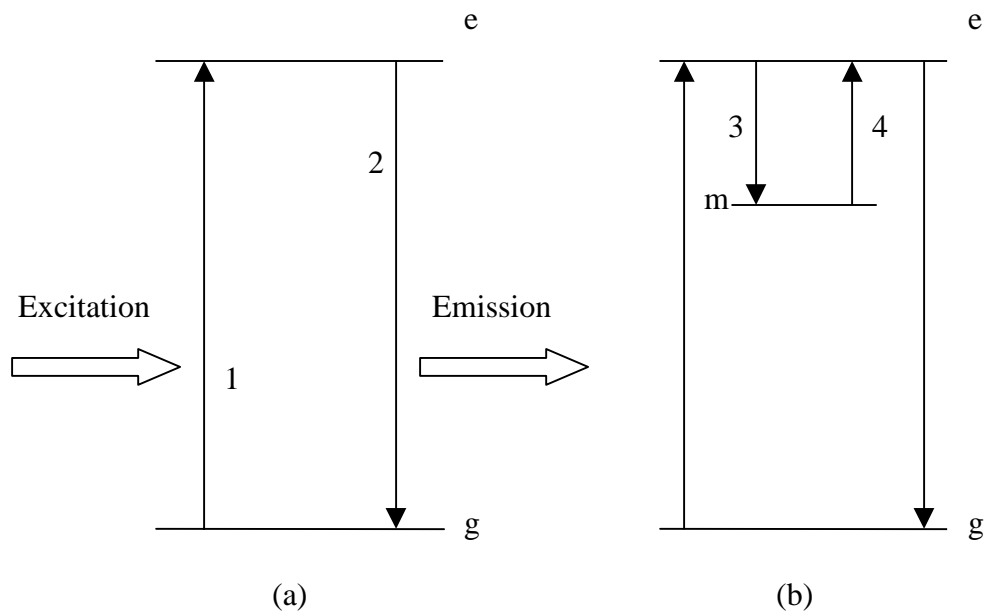


Figure 3.2. (a) Fluorescence (b) Phosphorescence

material, we will observe the thermoluminescence. Therefore, thermoluminescence is a special case of phosphorescence.

3.3 Simple Model for Thermoluminescence

For perfect lattice, the electron transitions only take place between energy bands, e.g. electrons in valence band are given enough energy to surmount an energy gap in order to be excited to the next higher energy band, i.e., conduction band, and electrons' return to the valence band will emit fluorescence. However, if there are impurities in the solid, some localized energy levels, which is formed in the energy gap, may be unoccupied, called traps (like a metastable state mentioned above). They have the capability of detaining the electrons that are supposed to return to the valence band, thereby delaying the luminescence (i.e. phosphorescence).

Based on the energy band model [27,28], the quantitative theory for thermoluminescence is developed [29,30,31,32]. A schematic representation of the simple model for thermoluminescence discussed by above pioneers is shown in figure 3.3. There are just two localized energy levels. One acts as trapping state (metastable state), which is close to the conduction band (T state in figure 3.3). The other one acts as recombination center (ground state), which is close to the valence band (R state).

When absorbing the energy from radiation, the electrons in valence band are excited to the conduction band (transition 1), producing free electrons in the conduction band and free holes in the valence band. The free holes may be tapped in the recombination center (transition 2) and the free electrons may become trapped in the trapping state (transition 3). From thermodynamic arguments, the average time spent by electrons in the trapping state at temperature T is given by:

$$\tau = s^{-1} \exp(E / kT) \quad (3.1)$$

Where, s is a constant (called frequency factor) and E is the energy difference between

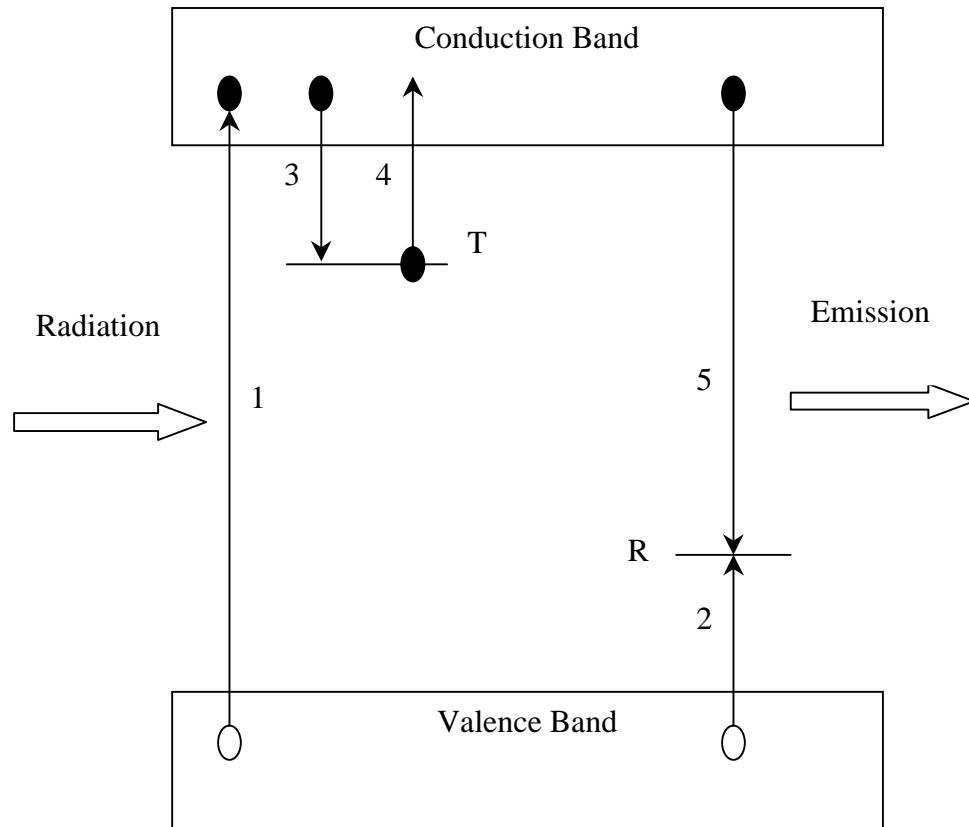


Figure 3.3. Simple model for thermoluminescence. Transition: (1) excitation; (2) hole trapping; (3) electron trapping; (4) thermal release; (5) recombination and light emission. Solid circle: electron; open circle: hole.

conduction band and trapping state (called the trap depth); k is Boltzmann's constant. We can rewrite this equation as follow:

$$p = \tau^{-1} = s \exp(-E / kT) \quad (3.2)$$

Here, p is defined as the probability per unit time of the release of an electron from the trap. All other terms remain as previously defined.

From equations (3.1) and (3.2), if the trap depth E is such that at the temperature of radiation, T_0 , $E \gg kT_0$, then any electron which becomes trapped will remain so for a long period of time. Even after removal of the radiation there will exist a substantial population of trapped electrons. Although the free electrons always have the trend to return to the conduction band (transition 4), the relaxation rate is very low and this metastable state will exist for an indefinite period. However, the rate can be increased by raising the temperature of the specimen above T_0 such that $E \leq kT$. Thus the probability of de-trapping p is increased and the electrons will be release from the trap into the conduction band. Thermoluminescence then results from the free electrons recombining with the trapped holes at the recombination center (transition 5).

3.4 Analysis of Simple Model

Randall & Wilkins gave the first thorough formalism for the simple model [31]. They assumed that once the electron had been freed from its trap (transition 4), the probability of it returning to the trap is much less than the probability of it returning to the recombination center (transition 5). The intensity of the thermoluminescence $I(t)$ at any time during the heating is proportional to the rate of recombination of trapped holes and electrons at level R . Hence,

$$I(t) = - dn / dt \quad (3.3)$$

Where n is the concentration of trapped electrons.

The relationship between $I(t)$ and n is shown schematically in figure 3.4. As the temperature rises the electrons are released and recombination takes place reducing the concentration of trapped holes and increasing the thermoluminescence intensity. As the electron traps are progressively emptied the rate of recombination decreases and thus the thermoluminescence intensity decreases accordingly. This produces the characteristic thermoluminescence peak at temperature T_m . Usually, in the experiment the temperature is raised as a linear function of time according to

$$T = T_0 + \beta t \quad (3.4)$$

Where, β is the heating rate given by dT/dt . Equation (3.4) is also displayed graphically in figure 3.4.

Because the probability of release of an electron from the trap is related to both the trap depth E and the temperature by equation (3.2), then the range of temperatures over which the thermoluminescence peak appears is related to the trap depth. For a given constant s , the larger the value of E (i.e. the deeper the trap), the higher the temperature T_m . In this way, a thermoluminescence experiment may provide some information on the distribution of trapping states.

The release of trapped electrons by thermal process also depends on the probability of their escaping given by equation (3.2). We can rewrite the equation (3.3) as

$$I(t) = -dn/dt = np = n s \exp(-E/kT) \quad (3.5)$$

Integrating above equation gives

$$n(t) = n_0 \exp \left[-s \int_{t_0}^t \exp(-E/kT) dt \right] \quad (3.6)$$

Where, n_0 is the number of electrons trapped at initial temperature T_0 . Use the linear heating function (equation (3.4)), we get

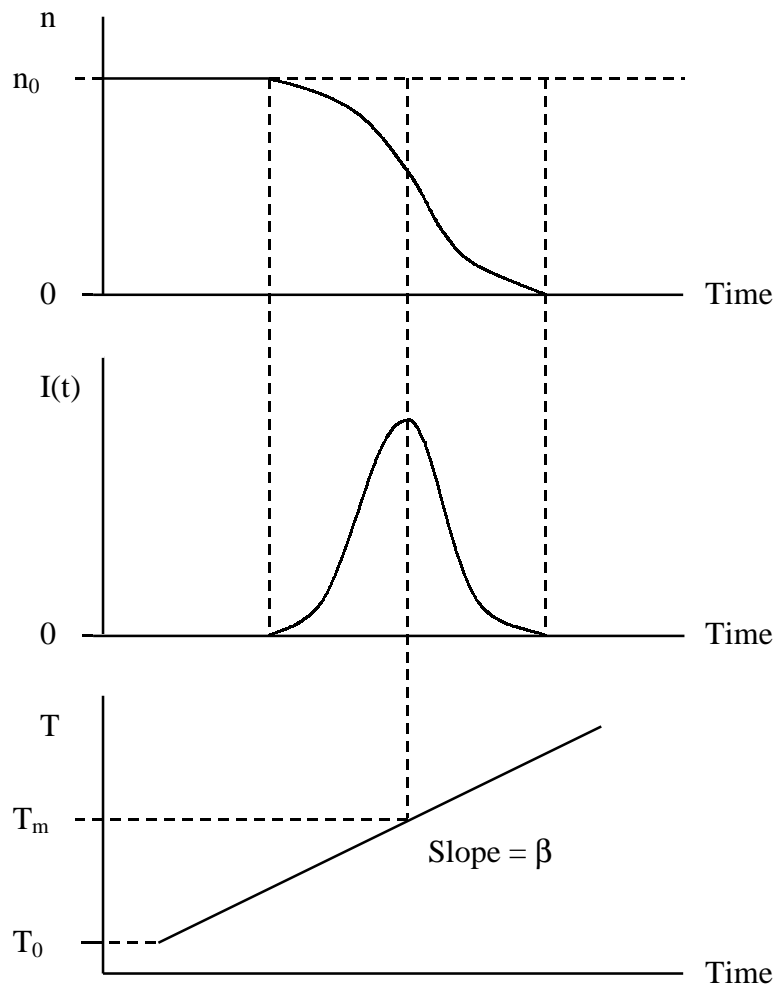


Figure 3.4. Relationship between thermoluminescence intensity $I(t)$ and the number of trapped electrons n . Also shown is the linear relation between time and temperature during heating.

$$n(t) = n_0 \exp \left[- \frac{s}{\beta} \int_{T_0}^T \exp(-E/kT) dT \right] \quad (3.7)$$

Inserting this expression in equation (3.5) yields

$$I(t) = n_0 s \exp(-E/kT) \exp \left[- s \int_{T_0}^t \exp(-E/kT) dt \right] \quad (3.8)$$

By setting $dI(t)/dT = 0$ at $T = T_m$, we obtain

$$\beta E / kT_m^2 = s \exp(-E/kT_m) \quad (3.9)$$

Using two different linear rates β_1 and β_2 and finding the corresponding peak temperatures T_{m1} and T_{m2} , respectively, and using equation (3.9) we can calculate the trap depth as:

$$E = \frac{kT_{m1}T_{m2}}{T_{m1} - T_{m2}} \ln \left[\frac{\beta_1}{\beta_2} \left(\frac{T_{m2}}{T_{m1}} \right)^2 \right] \quad (3.10)$$

This equation can be used to obtain the value of the trap depth energy E without determining the frequency factor s . Also, from equation (3.8), s can be calculated.

Furthermore, from equation (3.8) it is obvious that: (1) with the increase of β (heating rate), the T_m shifts to higher temperatures for a given trap [33]; and (2) for a constant value of β , T_m shifts toward higher temperatures as E increases or s decreases.

Therefore, we got the relationship among the trap depth energy E , the frequency factor s and the temperature. We could obtain the information about the impurity.

There have been many approaches to analyze the thermoluminescence phenomena. And of course, the model of actual specimen may be much more complex than the simple model. However, this simple model can explain, at least qualitatively, all the fundamental features of the thermoluminescence production. For further details of thermoluminescence, an excellent overview has been given by McKeever [9].

CHAPTER 4

THERMOLUMINESCENCE EXPERIMENT

4.1 Basic Idea

In figure 3.4 of chapter three, the thermoluminescence is displayed as a function of time. In experiment the normal way of displaying thermoluminescence data is to plot luminescence intensity as a function of temperature, known as a 'glow curve'. Figure 4.1 gives an example of glow curve. The peaks are due to different electron traps with different depths. Figure 4.2 displays the dependence of the thermoluminescence signal on the excitation wavelength. For different excitation wavelength, the thermoluminescence intensity is different. If we plot the integrated thermoluminescence signal as a function of excitation wavelength, we get the thermoluminescence excitation spectroscopy (TES). TES is form of excitation spectroscopy that probes the promotion of impurity electrons into the conduction band. Using tunable visible and UV radiation we determine the threshold for trap filling, which coincides with the ionization threshold of a specific impurity. The basic idea of this technique is shown in figure 4.3. At the beginning, the sample is heated to high temperature to empty traps; then it is cooled to the low temperature and exposed at a fixed energy $h\nu_E$ for give period of time. If the energy of the radiation is high enough to surmount the energy gap E_{PI} between the impurity ground state and the conduction band CB (solid arrow, figure 4.3a), The electrons of impurity are excited to the conduction band; a small fraction of the free electrons will be trapped. If the energy of the radiation is too small to surmount the energy gap (dashed arrow, figure 4.3a), no electron transfer process occurs and the traps remain empty. After exposure the sample is heated rapidly. If the traps had been filled during exposure, trapped electrons

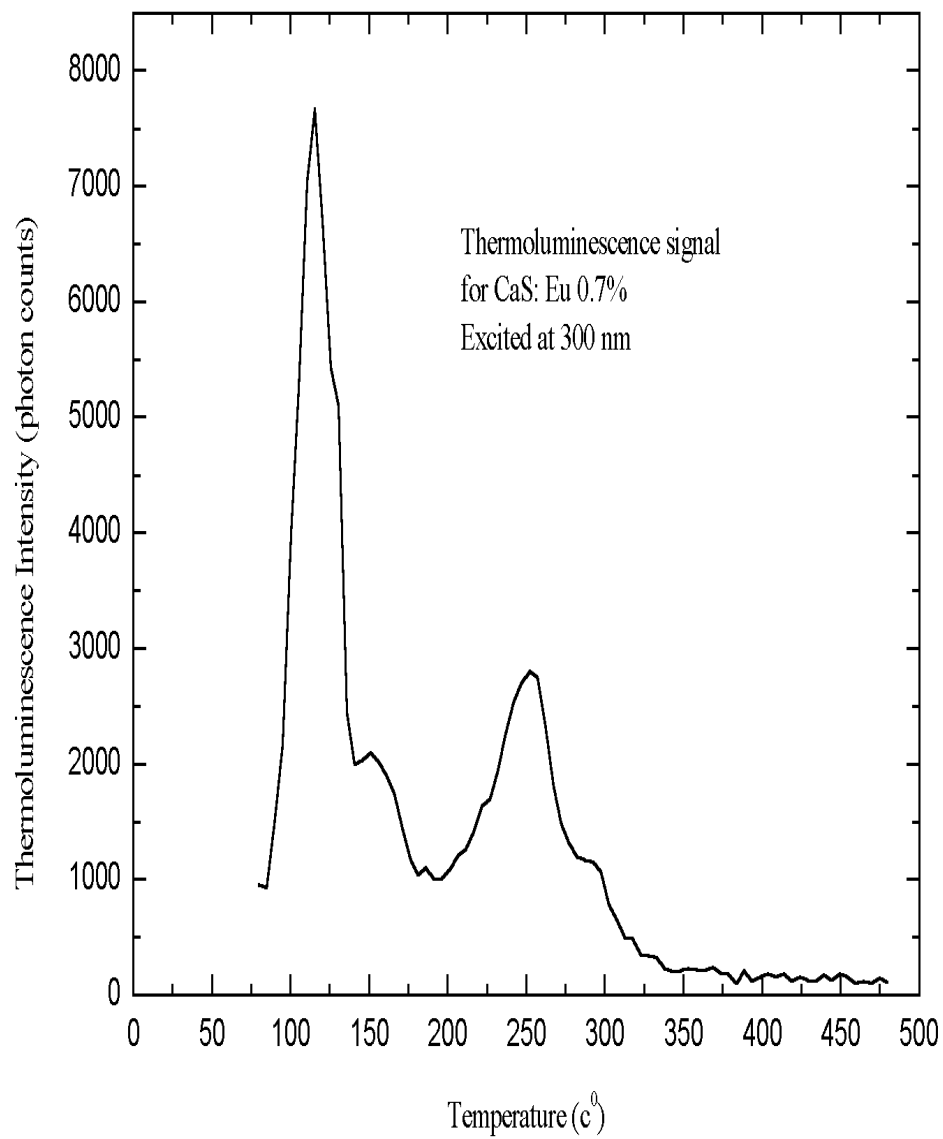


Figure 4.1. Glow curve: Thermoluminescence intensity as the function of temperature

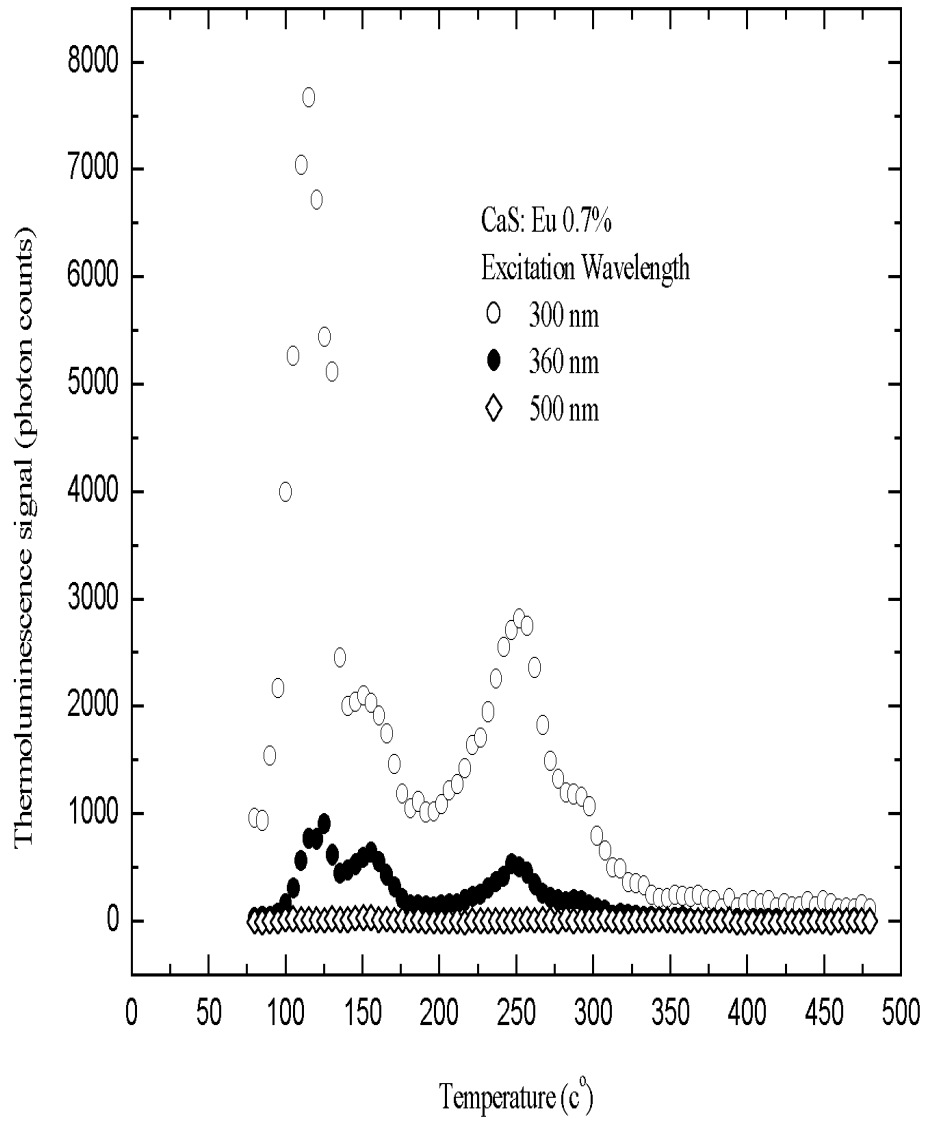


Figure 4.2. Thermoluminescence signal for CaS: Eu powder; shows the dependence on the excitation wavelength.

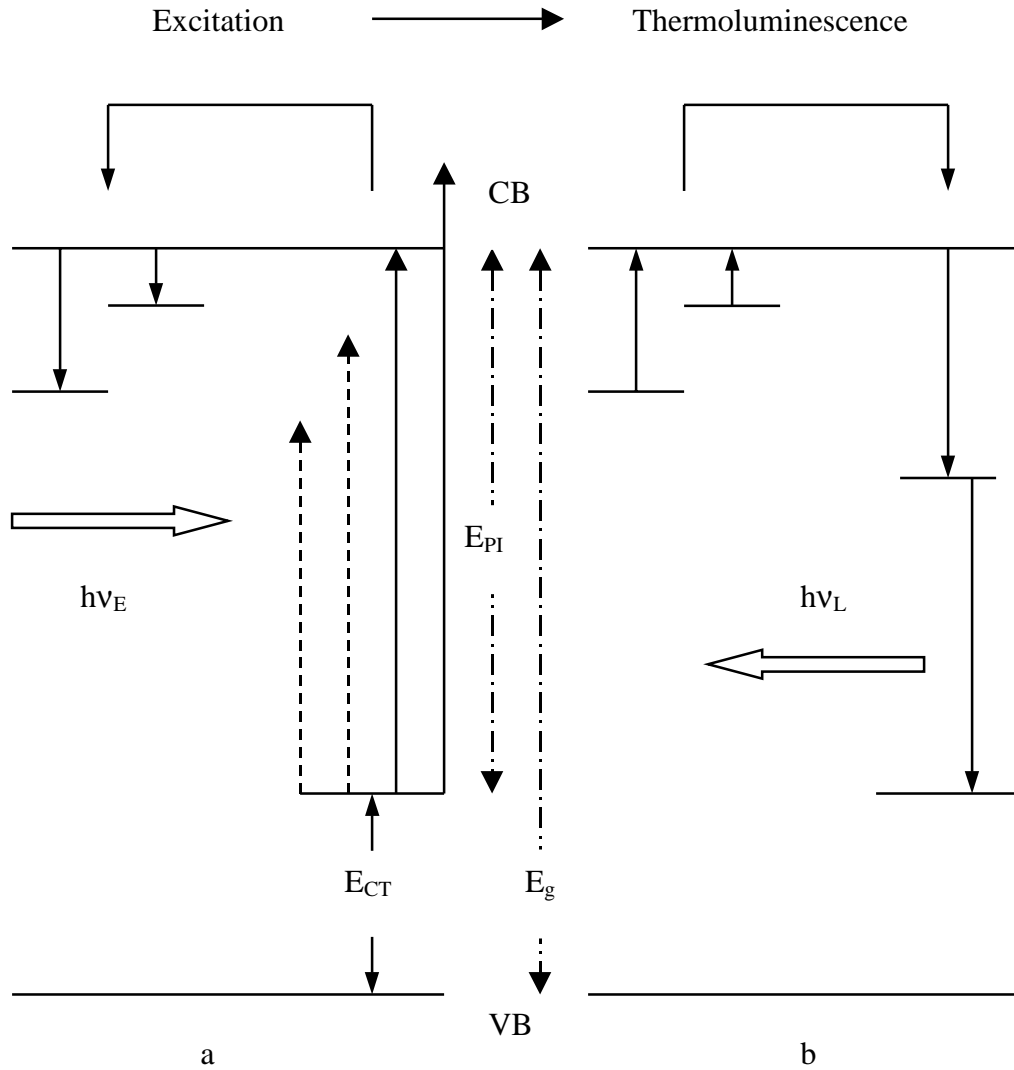


Figure 4.3. The principle of using thermoluminescence to locate the ground state of impurity. Thermoluminescence spectroscopy determines the onset of trap filling which gives the ionization energy E_{PI} (or E_{CT}).

are released due to the thermal activation and recombine with the ionized impurities, with subsequent emission of impurity specific radiation at $h\nu_L$, i.e. thermoluminescence is observed (figure 4.3b). The cycle is then repeated, exposing the sample at a different wavelength. Plotting the integrated thermoluminescence signal as a function of excitation wavelength then gives the ionization threshold of the impurity ion. Likewise, the threshold E_{CT} for charge transfer transitions can be determined.

4.2 Experimental Setup and Procedure

The schematic representation of experimental setup is shown in figure 4.4. The sample is mounted on a coldfinger that is made of copper because of its good conductivity. The coldfinger is cooled by liquid nitrogen, which makes a rapid cooling of the sample by about 10-15 minutes. Since to get the thermoluminescence needs heat the sample, also the coldfinger is equipped with a high power heater to rapidly ramp the sample temperature from the base temperature of 77 K to up to 600 K. The coldfinger is placed in a cryostat and is under vacuum. When the sample is at the low temperature, the radiation is applied. We use a 100 W Xenon lamp or a 30 W Deuterium lamp as the radiation source, filtered by a 0.125 m monochromator. After the exposure at the low temperature, the lamp is turned off and a temperature controller ramps the temperature of the coldfinger. During the heating of sample at a constant heating rate, the thermoluminescence is recorded by a light sensitive detector. We use a photomultiplier tube with a narrow band filter, which is used to select the detection wavelength. The photomultiplier is connected to a photo-counting system that records the thermoluminescence signal as a function of sample temperature. As an alternative, the entire thermoluminescence spectrum can be recorded by a CCD camera, mounted onto a monochromator. Now we can see the whole procedure of observing thermoluminescence requires a cooling, exposure and heating cycle. Like mentioned in chapter three, this

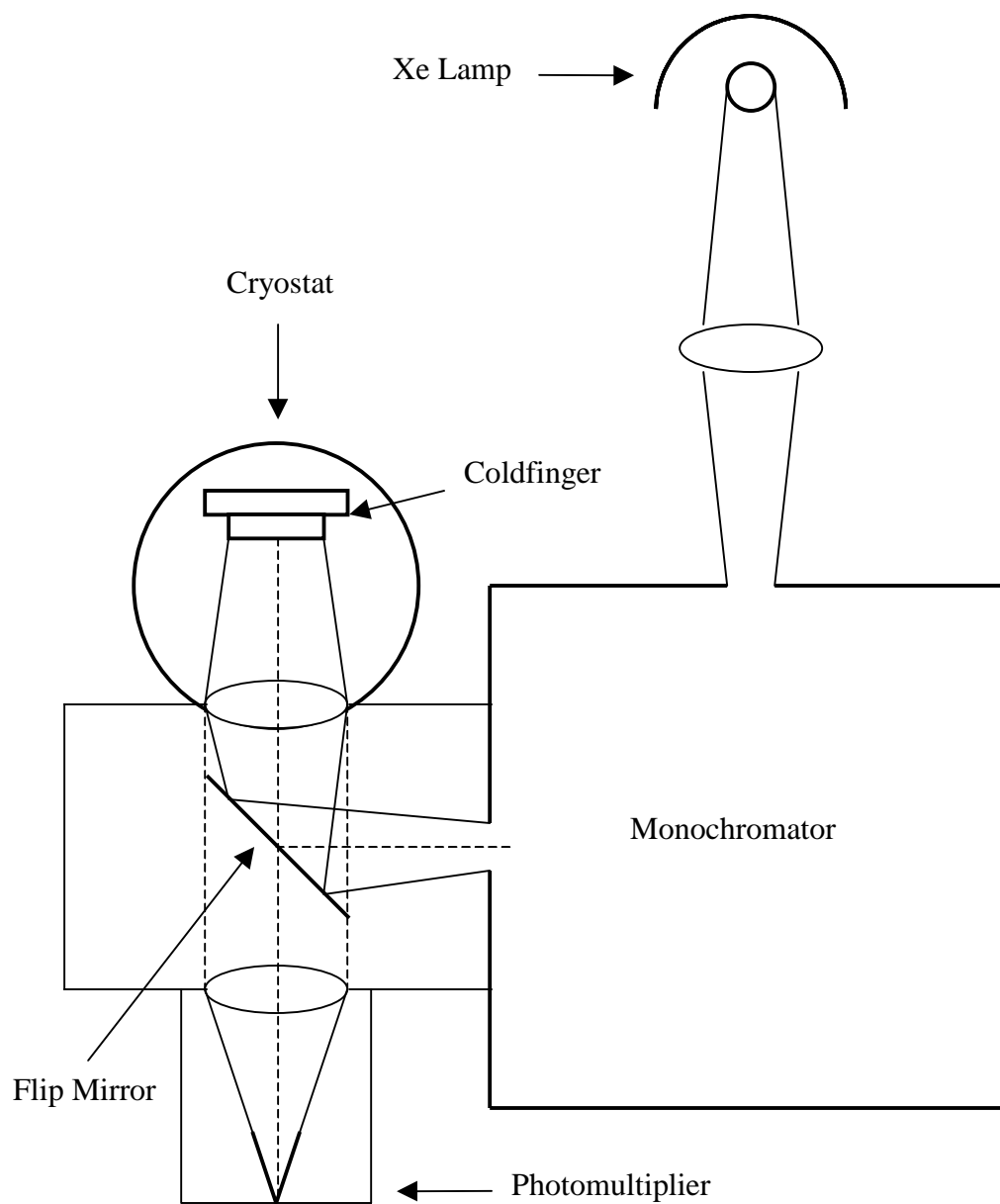


Figure 4.4. The layout for thermoluminescence experiment

procedure is a “one shot” effect. We have to repeat the cycle at each excitation wavelength. The shortest cycle time is about 30 minutes, but must often be extended to an hour if longer exposure and/or heating to very high temperature are required.

4.3. Experimental Results

4.3.1 Single Crystal: $\text{Y}_2\text{SiO}_5: \text{Ce}^{3+}$.

The energy level diagram for trivalent cerium is simple, since it is a one-electron case. The $4f^1$ ground state splits into $^2F_{5/2}$ and $^2F_{7/2}$ states due to spin-orbit coupling [34]. The next higher level is 5d state, which is split by crystal field into 2 to 5 components [1]. The 4f-5d transitions are allowed by the parity selection rule.

In $\text{Y}_2\text{SiO}_5: \text{Ce}^{3+}$, oxygen vacancies act as the electrons trap, and Ce^{3+} ions act as holes trap (recombination center) [35]. After exposure at low temperature, when heating the sample to empty the electron trap, the release electron recombines with a hole trapped on Ce^{3+} , resulting in Ce^{3+} in the excited state. Ce^{3+} returns to the ground state giving the $5d \rightarrow 4f$ light emission. The model suggested above is shown schematically in figure 4.5. The entire thermoluminescence spectrum of $\text{Y}_2\text{SiO}_5: \text{Ce}^{3+}$ excited at 280nm, recorded by CCD camera, is shown in figure 4.6. The emission is a broad band with peaks around 400nm and 440 nm (due to the ground state splitting). Figure 4.7 and figure 4.8 show the thermoluminescence excitation spectra (TES) of $\text{Y}_2\text{SiO}_5: \text{Ce}^{3+}$. The ionization threshold is evident. The signal raises sharply around 330 nm, which we interpret as the ionization threshold of Ce^{3+} in this material. This result is in excellent agreement with our photoconductivity experiments, which also gives an ionization threshold around 330 nm [36]. Figure 4.9 displays the photoconductivity spectra of $\text{Y}_2\text{SiO}_5: \text{Ce}^{3+}$ at different temperatures. At low temperature ($T = 80\text{K}$), the threshold is at about 330nm.

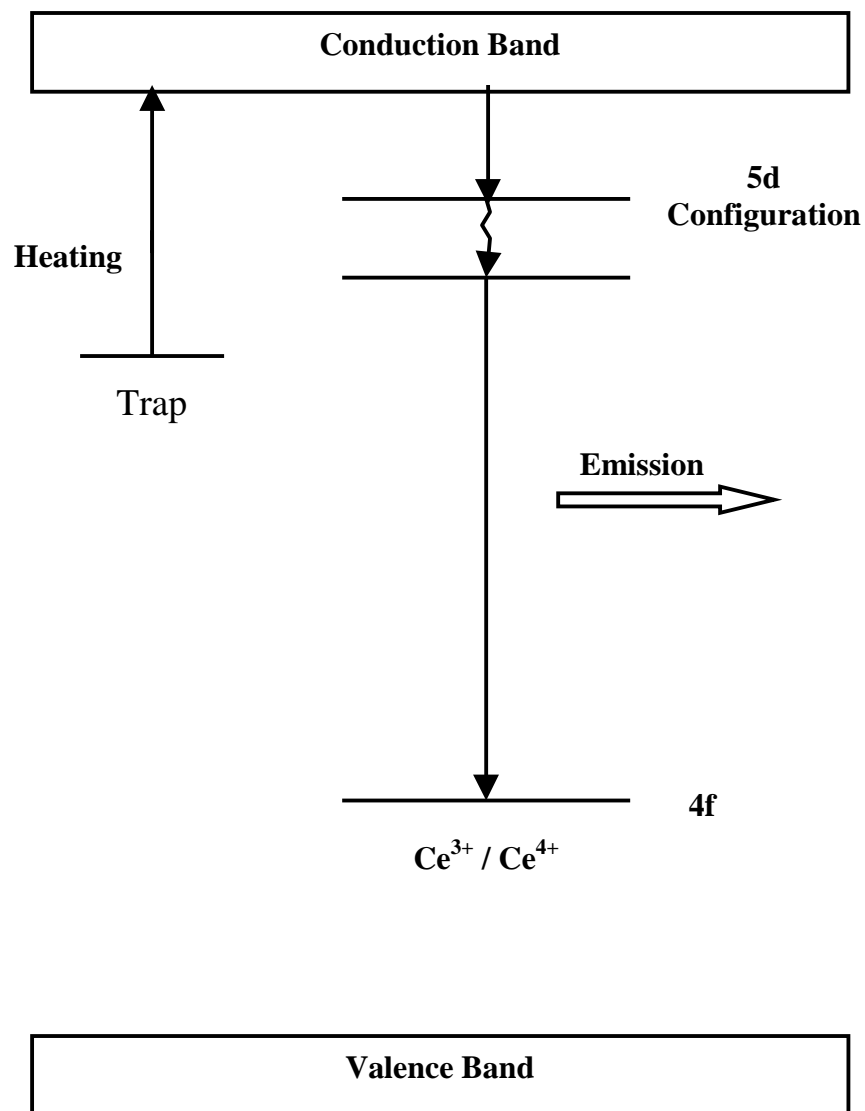


Figure 4.5. Schematic representation of the model suggested for recombination in $\text{Y}_2\text{SiO}_5: \text{Ce}^{3+}$.

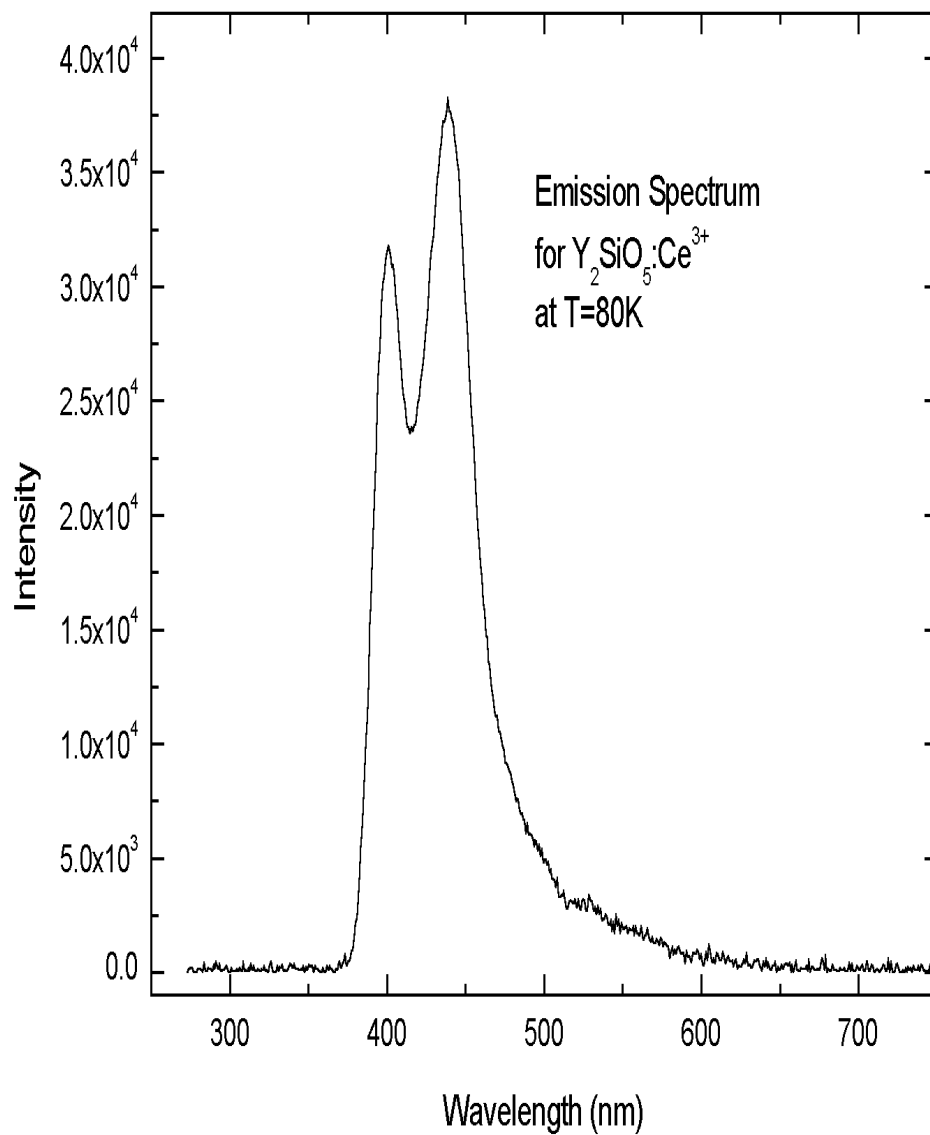


Figure 4.6. The emission spectrum of $\text{Y}_2\text{SiO}_5:\text{Ce}^{3+}$ at low temperature $T=80\text{K}$ record by CCD camera.

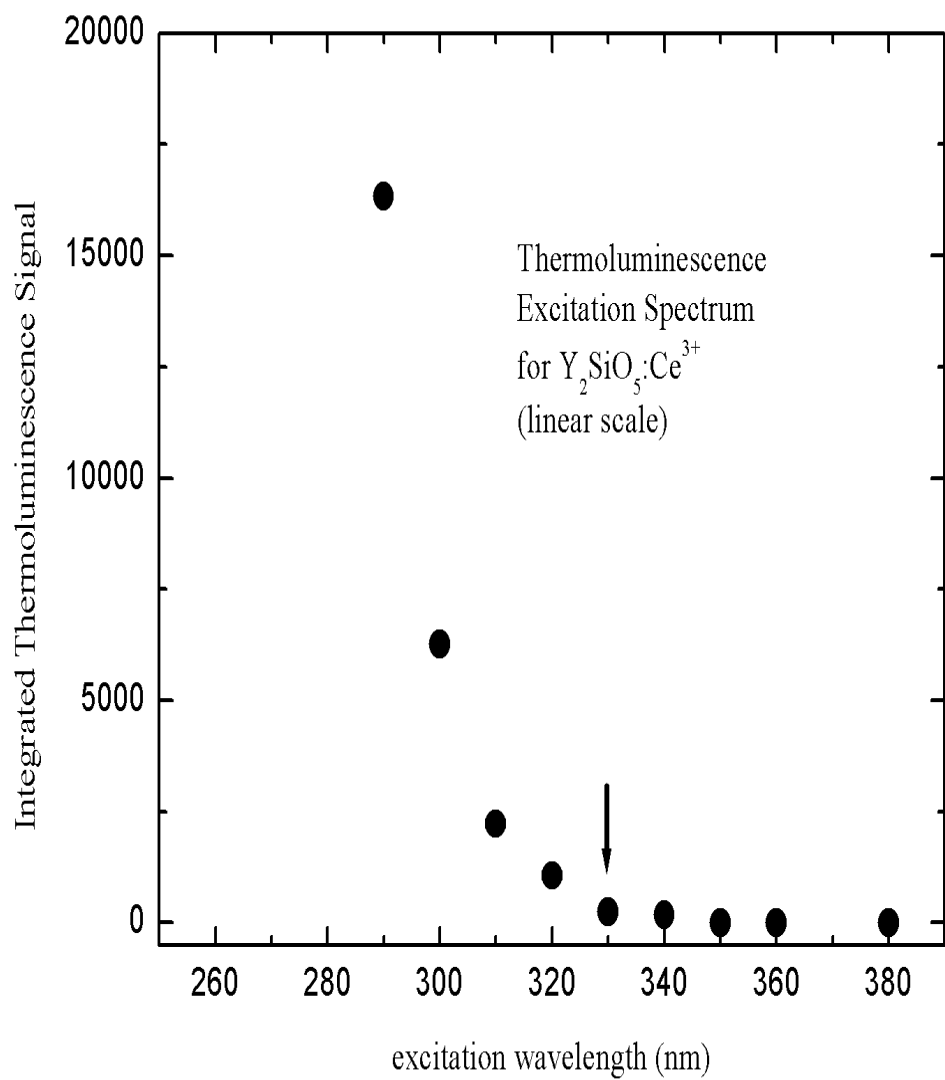


Figure 4.7. Thermoluminescence excitation spectrum for single crystal $Y_2SiO_5:Ce^{3+}$ in linear scale.

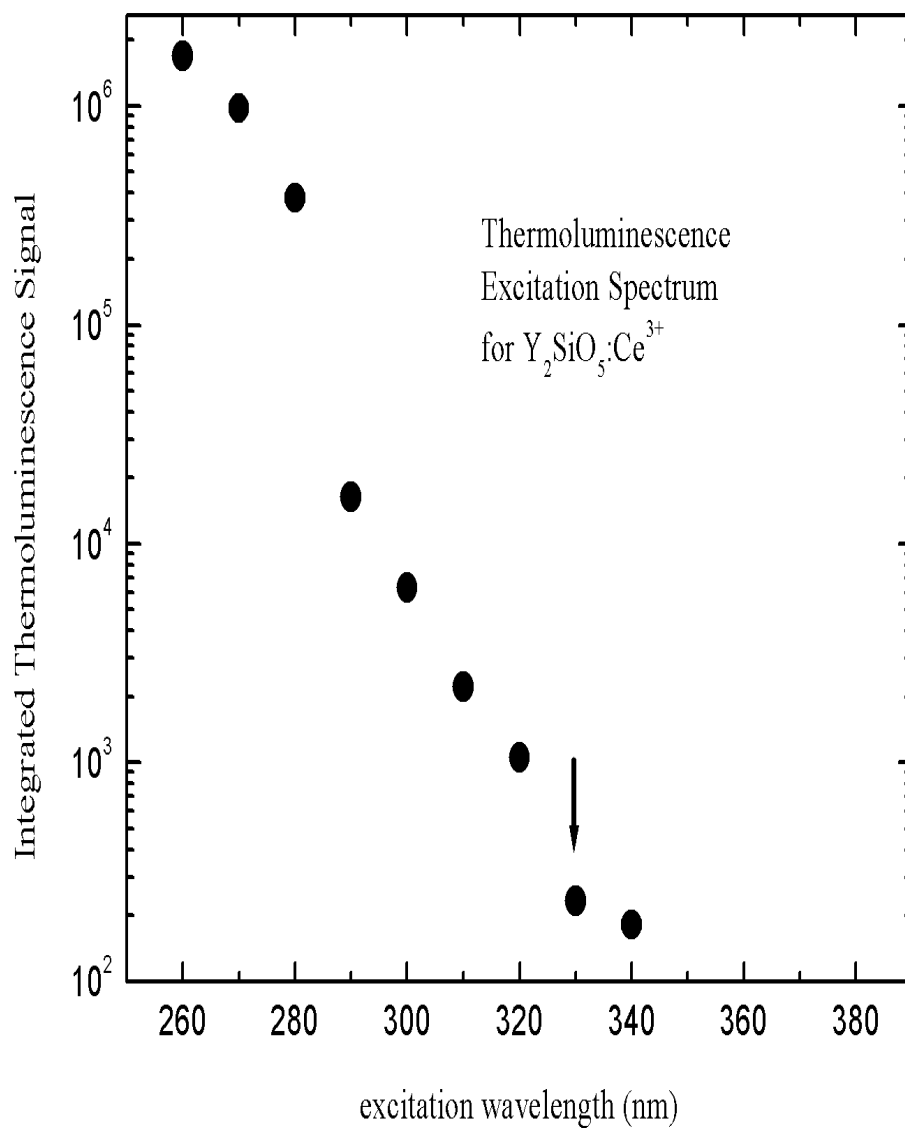


Figure 4.8. Thermoluminescence excitation spectrum for single crystal $\text{Y}_2\text{SiO}_5:\text{Ce}^{3+}$ in logarithmic scale.

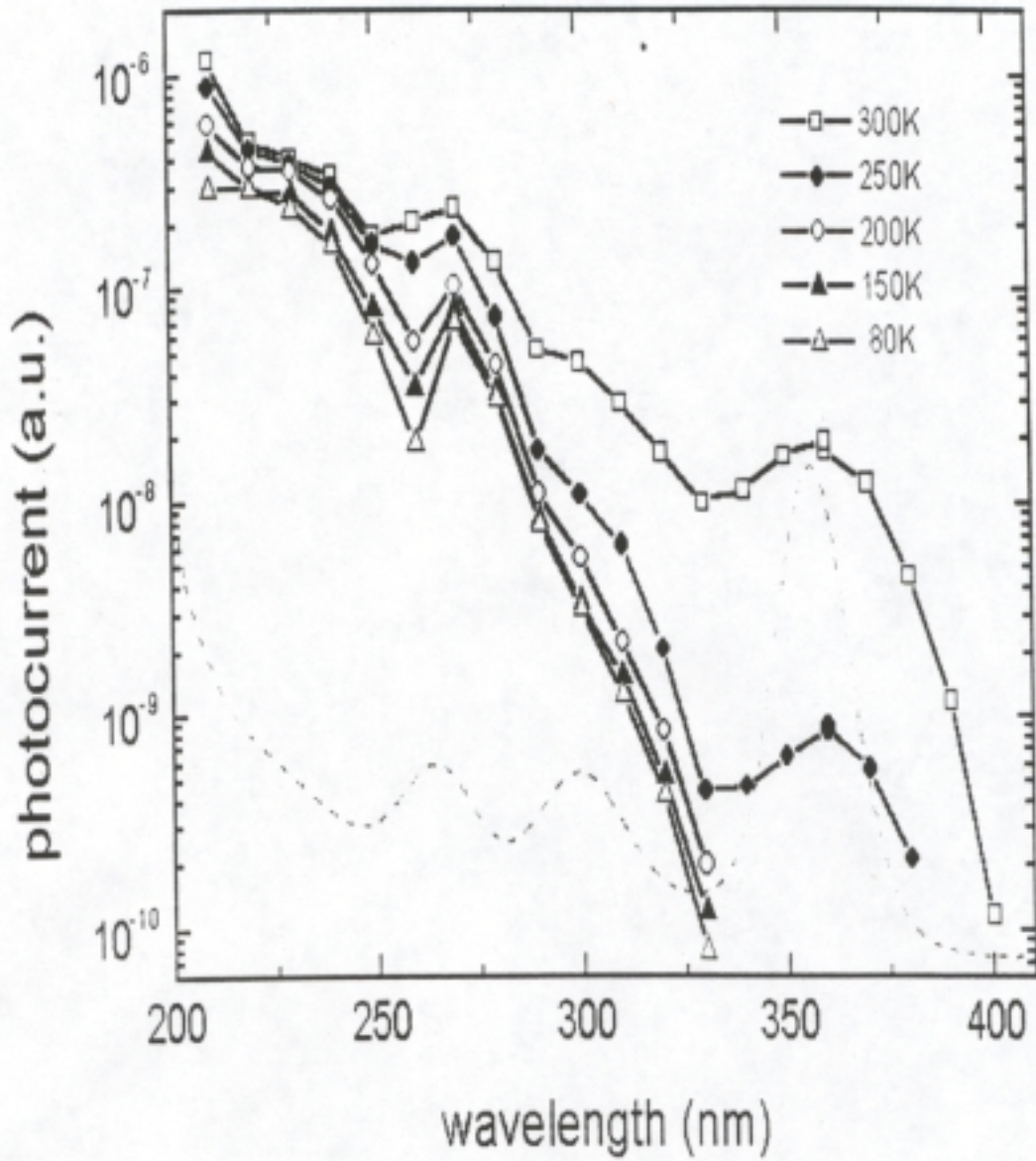


Figure 4.9. Photoconductivity spectrum of Y₂SiO₅: Ce³⁺ at different temperatures. The dotted line is the absorption spectrum.

4.3.2 Microcrystalline Material: CaS: Eu²⁺

This sample is microcrystalline powder CaS: Eu²⁺. The energy levels of Eu²⁺ are shown in figure 4.10. The thermoluminescence signal is because the transition from 4f⁶5d excited state to 4f⁷ state. The figure 4.11 shows the TES spectrum when the sample was irradiated at T=80K. We find one threshold at 500 nm. In the chapter two, the figure 2.5 shows the photoconductive spectra of CaS: Eu²⁺ at different temperatures. Comparing our results with those obtained via photoconductivity, we see that at low temperature (T=80K), the photoconductive spectrum displays two thresholds, one around 510 nm and the second around 650 nm. The higher energy threshold (510nm) is attributed to the ionization of Eu²⁺ ions, which agrees with our results. The lower energy threshold is because of the tunneling of electron between Eu²⁺ and Eu³⁺ ions [22,37]. This process should not result in thermoluminescence signal. Again, our results confirm this point for observing only one threshold.

4.3.3 Ce³⁺ Doped Li-Mg-Silicate Glass

The last sample is Ce³⁺doped Li-Mg-Silicate glass. Figure 4.12 is the TES spectrum. We find a strong rise of the signal at 280 nm, which can be interpreted as the ionization threshold. It has to be pointed out that this interpretation is preliminary. However, the photoexcitation spectrum of the glass (figure 4.13, detecting wavelength 440nm) shows no structure around 280 nm due to band-to-band absorption, giving support to our tentative assignment of the ionization threshold for Ce³⁺ ion in this material.

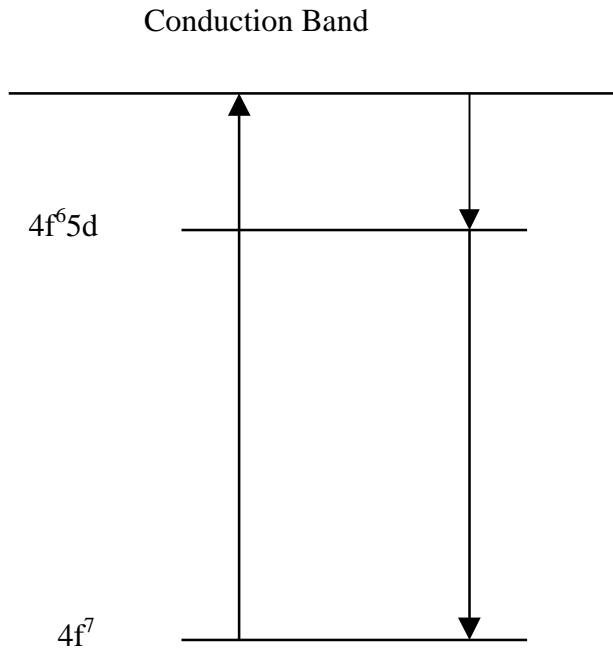


Figure 4.10. The energy levels of CaS:Eu^{2+}

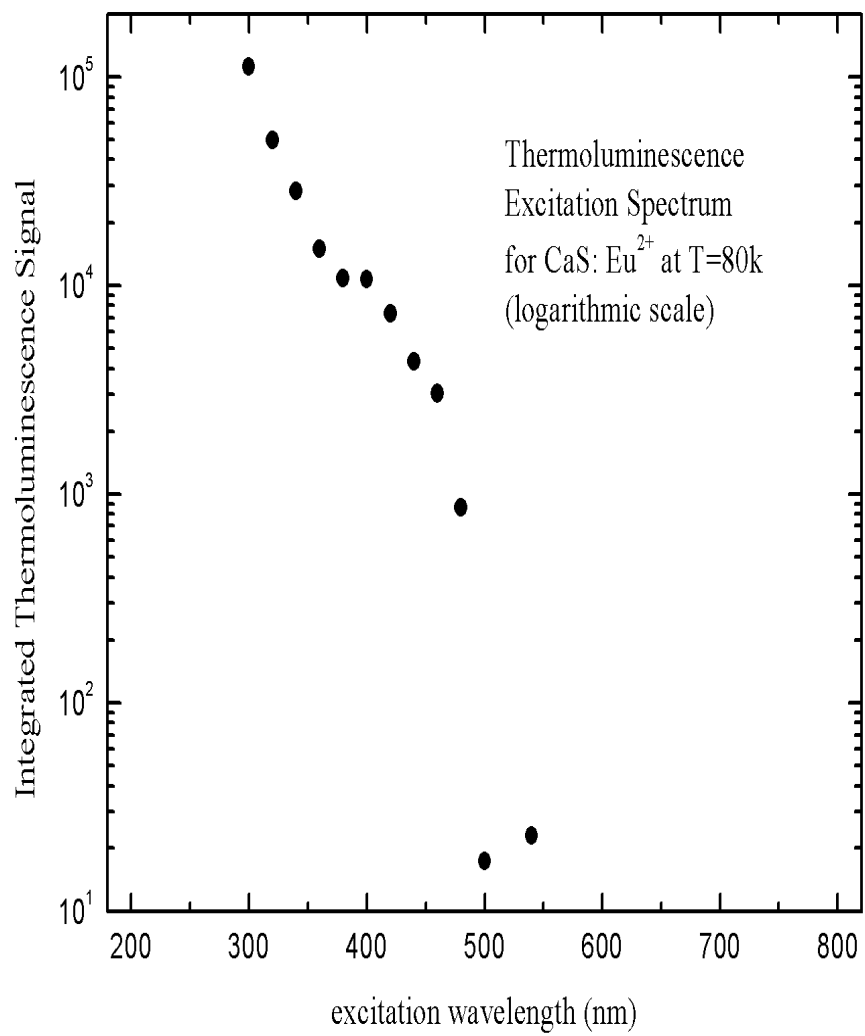


Figure 4.11. Thermoluminescence excitation spectrum of CaS: Eu²⁺ microcrystalline powder.

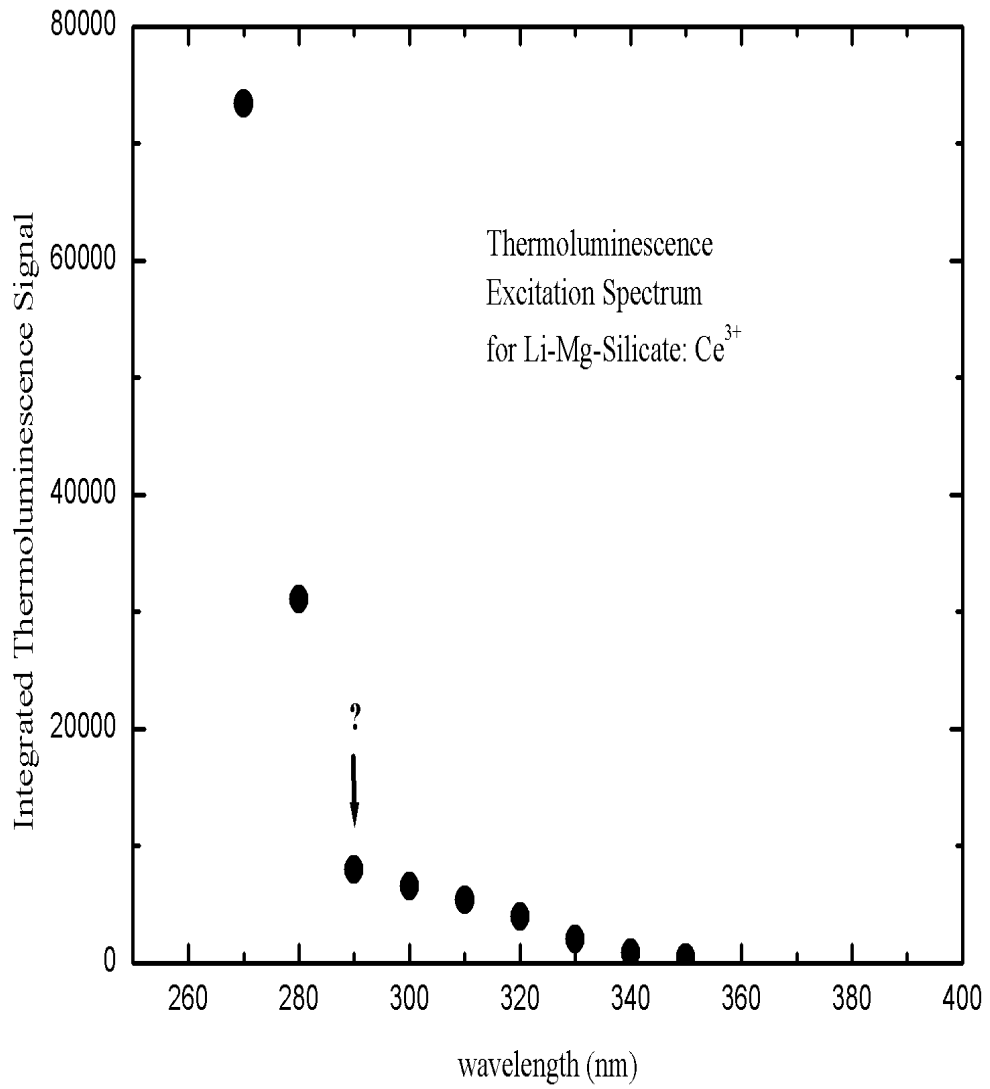


Figure 4.12. Thermoluminescence excitation spectrum of Li-Mg-Silicate glass doped with Ce³⁺.

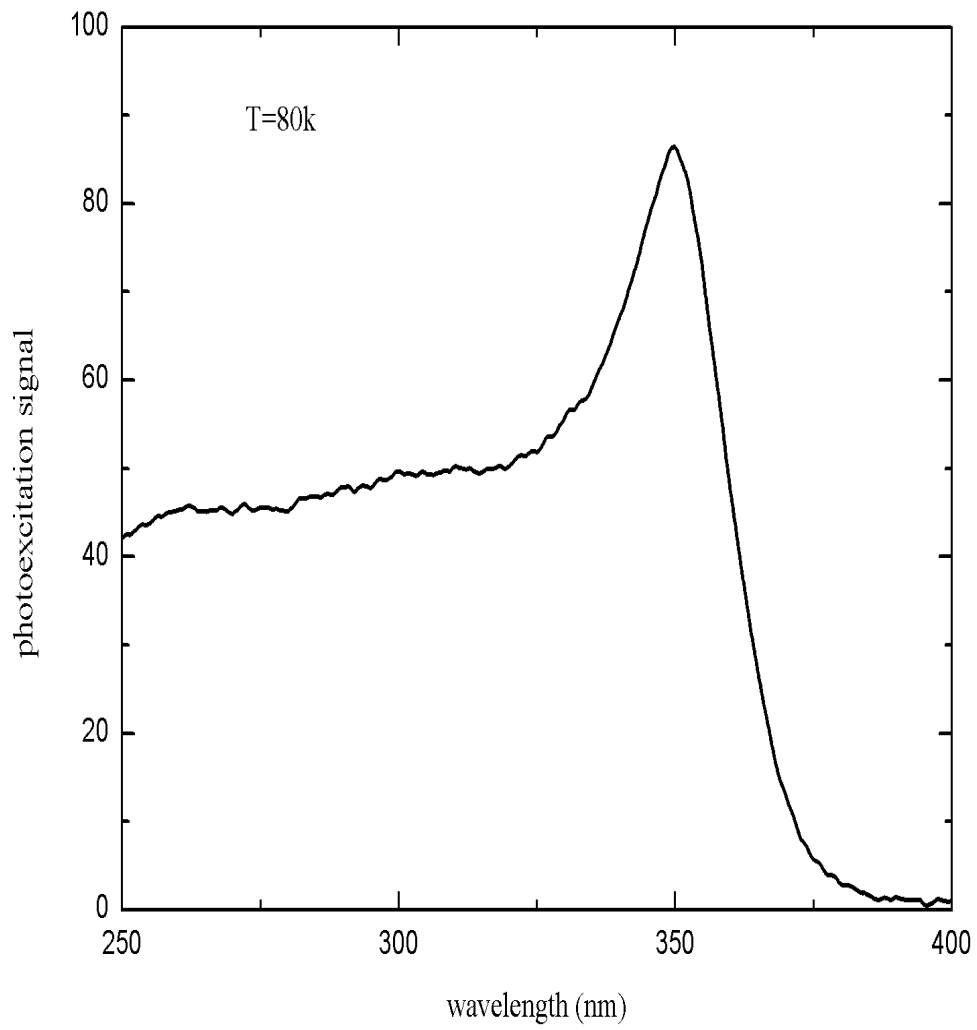


Figure 4.13. Photoexcitation spectrum of Li-Mg-Silicate glass doped with Ce^{3+} .

CHAPTER 5

CONCLUSIONS

This thesis presents thermoluminescence as a technique to study the energy levels of impurity in solid. The examples shown demonstrate that the thermoluminescence excitation spectroscopy (TES) is an excellent technique to obtain the ionization threshold of impurity ions in insulating materials. The advantages of TES include:

Impurity and impurity site specific signal. A major advantage of this technique is the impurity specific signal, that is, the thermoluminescence signal is characteristic for the impurity or site.

Electron and hole specific thermoluminescence signal. The thermoluminescence signal as a function of temperature depends on the trap depth. Since hole traps differ from electron traps, TES gives the opportunity to distinguish between photoionization and charge transfer processes. Combination of TES and photoconductivity measurements then allows one to distinguish between electron and hole conductivity. This application is important for doped insulators, where attempts to conduct Hall measurements are generally futile.

Experiments on single crystals, ceramic samples, and microcrystalline powder. TES can be easily applied to ceramic samples and microcrystalline or nanocrystalline particles.

For our experimental setup, a complete spectrum can be obtained within 1 day. Complementing with other techniques like photoconductivity technique, standard absorption and photoexcitation techniques, the TES approach will be a power tool. The

systematic study of the position of impurity energy levels with respect to the host valence and conduction bands are under way.

REFERENCES

1. G. Blasse, B. C. Grabmaier, *Luminescent Materials*, Springer, Berlin, 1994.
2. B. Henderson, G. F. Imbusch, *Optical Spectroscopy of Inorganic Solids*, Clarendon Press, Oxford, 1989.
3. J. I. Pankove, *Optical Processes in Semiconductors*, Prentice Hall, Inc. Englewood Cliffs, NJ, 1971.
4. Kital AH (ed) *Solid State Luminescence. Theory Materials and Devices*, Chapman and Hall, 1993.
5. C. Kunz (Ed.), *Synchrotron Radiation; Techniques and Applications*, Topics in Current Physics, Vol. 10, Springer-Verlag, Berlin, 1979.
6. J. Choi, S. A. Basun, L. Lu, W. M. Yen and U. Happek, *J. Lumin.* 83-84 (1999) 461.
7. W.M. Yen, M. Raukas, S. A. Basun, W. van Schaik, U. Happek, *J. Lumin.* 69 (1996) 287.
8. J. Choi, S. A. Basun, R. S. Meltzer, M. Raukas, J. Rennie, J. C. Vial, W. M. Yen, P.N. Yocom, U. Happek, *J. SID, Supplement-1*, (2000) 193.
9. S. W. S. McKeever, *Thermoluminescence of Solids*, Cambridge University Press, Cambridge, New York, 1985.
10. C. Kittel, *Introduction to Solid State Physics*, John Wiley & Sons, Inc., New York, London, Sydney, 1966.
11. R. H. Bube, *Photoconductivity of Solids*, J. Wiley & Sons, New York London, 1960.
12. M. Born, *Verh. Dtsch. Phys. Ges.* 21 (1919) 679.
13. F. Haber, *Verh. Dtsch. Phys. Ges.* 21 (1919) 750.

14. W. C. Wong, D. S. McClure, S. A. Basun, M. R. Kokta, *Phys. Rev. B* 51 (1995) 5682.
15. Stefan Hufner, *Photoelectron Spectroscopy: Principles and Applications*. Springer-Verlag, Berlin, 1996.
16. H. Hertz, *Ann. Physik* 31, 983 (1887).
17. Einstein, *Ann Physik* 17, 132 (1905).
18. W. Smith, *Nature* 7, 303 (1873).
19. Rose, *Concepts in Photoconductivity and Allied Problems*, Interscience Publishers, New York, 1963
20. D. S. McClure, C. Pedrini, *Phys. Rev. B* 32 (1985) 8465.
21. C. Pedrini, F. Rogemond, D. S. McClure, *J. Appl. Phys.* 59 (1986).
22. U. Happek, S. A. Basun, J. Choi, J. K. Krebs, M. Raukas, *J. Alloys and Compounds*. 303 (2000) 198.
23. E. Wiedemann, G. C. Schmidt, *Ann. Phys. Chem. Neue Folge*, 54 (1895) 604.
24. G. F. J. Garlick, *Luminescent Materials*, Oxford University Press, London, 1949.
25. D. Curie, *Luminescence in Crystals*, Methuen, London, 1960.
26. Jablonski, *Z. Phys.* 94 (1935) 38.
27. R. P. Johnson, *J. Opt. Soc. Am.*, 29 (1939) 387.
28. F. E. Williams, *J. Opt. Soc. Am.*, 39 (1949) 648.
29. G. F. J. Garlick, M. H. F. Wilkins, *Proc. Roy. Soc. Lond.*, 184 (1945) 408.
30. J. T. Randall, M. H. F. Wilkins, *Proc. Roy. Soc. Lond.*, 184 (1945) 366.
31. J. T. Randall, M. H. F. Wilkins, *Proc. Roy. Soc. Lond.*, 184 (1945) 390.
32. G. F. J. Garlick, A. F. Gibson, *Proc. Phys. Soc.*, 60 (1948) 574.
33. P. Braunlich, *J. Appl. Phys.* 38 (1967) 1221, 2516
34. R. Lang, *Can. J. Res.* 14A (1936) 127.
35. Meijerink, W. J. Schipper, G. Blasse, *J. Phys. D: Appl. Phys.* 24 (1991) 997.

36. J. Choi, Dissertation, The University of Georgia, Athens, GA., 2001
37. S. A. Basun et al., Phys. Rev. B56 (1997) 1299
38. D. R. Vij (Ed.), Luminescence of Solids, Plenum Press, New York and London, 1998.
39. C. Pedrini, D. S. McClure, C. H. Anderson, J. Chem. Phys. 70(11) (1979) 4959